Sirtuin-3 (Sirt3) regulates skeletal muscle metabolism and insulin signaling via altered mitochondrial oxidation and reactive oxygen species production

Enxuan Jing[a], Brice Emanuelli[a], Matthew D. Hirschey[b,c], Jeremie Boucher[a], Kevin Y. Lee[a], David Lombard[d,1], Eric M. Verdin[b,c], and C. Ronald Kahn[a,2]

[a]Joslin Diabetes Center, Harvard Medical School, Boston, MA 02215; [b]Gladstone Institute of Virology and Immunology, San Francisco, CA 94158; [c]University of California, San Francisco, CA 94143; and [d]Department of Genetics, Harvard Medical School, Boston, MA

Contributed by C. Ronald Kahn, July 20, 2011 (sent for review April 14, 2011)

Sirt3 **is a member of the sirtuin family of protein deacetylases that is localized in mitochondria and regulates mitochondrial function.** ***Sirt3*** **expression in skeletal muscle is decreased in models of type 1 and type 2 diabetes and regulated by feeding, fasting, and caloric restriction.** ***Sirt3*** **knockout mice exhibit decreased oxygen consumption and develop oxidative stress in skeletal muscle, leading to JNK activation and impaired insulin signaling. This effect is mimicked by knockdown of** ***Sirt3*** **in cultured myoblasts, which exhibit reduced mitochondrial oxidation, increased reactive oxygen species, activation of JNK, increased serine and decreased tyrosine phosphorylation of IRS-1, and decreased insulin signaling. Thus,** ***Sirt3*** **plays an important role in diabetes through regulation of mitochondrial oxidation, reactive oxygen species production, and insulin resistance in skeletal muscle.**

mitochondrial metabolism | protein acetylation

Insulin resistance in skeletal muscle is a major and early feature in the pathogenesis of type 2 diabetes (1, 2). This pathological condition has been shown to involve decreased activity of the insulin signaling network with reduced tyrosine phosphorylation of the insulin receptor and its substrates, decreased activation of phosphatidylinositol 3-kinase (PI 3-kinase), and decreased activation of Akt/PKB (protein kinase B), leading to reduced glucose uptake and other metabolic abnormalities (3–5). Another early feature of type 2 diabetes is altered mitochondrial function in muscle. Reduced expression of multiple nuclear-encoded genes involved in mitochondrial oxidative phosphorylation and alterations in mitochondrial morphology have been observed in skeletal muscle of both rodent models of diabetes and humans with type 2 diabetes (6–8). Impaired mitochondrial lipid oxidation and glycolytic capacity have also been observed in individuals with diabetes and obesity, whereas enhanced mitochondrial lipid oxidation capacity has been associated with improved insulin resistance (9, 10). This reduced expression and/or activity of mitochondrial proteins has been closely associated with altered skeletal muscle physiology and metabolism. Some, but not all, studies have found similar alterations in skeletal muscle of individuals with a family history positive for type 2 diabetes (8, 11). Reduced oxidative capacity and reduced ATP synthesis rates have also been shown in individuals with type 2 diabetes and in some nondiabetic individuals with a family history for diabetes (12).

In addition to its role in substrate metabolism, the mitochondrion is the major production site of reactive oxygen species (ROS). When ROS level is excessive or there is impaired ROS clearance, the oxidative stress response can activate serine/threonine kinases such as protein kinase C, S6 kinase, and Jun N-terminal kinase (JNK), which can phosphorylate the insulin receptor (IR) and/or insulin receptor substrate (IRS) proteins (13–15), leading to a decrease in their tyrosine phosphorylation, decreased activation of PI 3-kinase and Akt, and resistance to the metabolic actions of insulin. Collectively, these data suggest that altered mitochondrial oxidative phosphorylation may be an early, or even primary, contributor to development of skeletal muscle insulin resistance and type 2 diabetes.

In recent years, the sirtuin family of NAD^+-dependent deacetylases has emerged as important regulators of metabolism. Among seven members of the sirtuin family, *Sirt3* is of particular interest with regard to mitochondrial function because it is localized primarily in mitochondria (16). *Sirt3* has been shown to deacetylate and thereby regulate several mitochondrial targets, including acetyl-CoA synthase 2 and glutamate dehydrogenase (17, 18). It has been suggested that *Sirt3* is also closely involved in energy homeostasis and regulation of ATP production in various tissues (19). Recently, we have shown that *Sirt3* plays an important role in hepatic lipid metabolism (20). Through these and other effects, Sirt3 has been shown to be involved in mitochondrial function and is associated with aging (21, 22).

We previously found that *Sirt3* expression is significantly decreased in muscle of mice with insulin-deficient diabetes (23), suggesting that decreased Sirt3 activity could contribute to the metabolic abnormalities of diabetes. In the present study, we demonstrate that skeletal muscle *Sirt3* expression is altered in models of both type 1 and type 2 diabetes and that alteration in *Sirt3* expression regulates mitochondrial metabolism and production of ROS, which in turn alters insulin signaling. These findings suggest a broad-reaching role of *Sirt3* in altered muscle metabolism in both normal and diabetic states.

Results

Changes in *Sirt3* Expression in Models of Diabetes and Aging. Quantitative PCR using muscle from streptozotocin (STZ) diabetic mice revealed an ~50% decrease of *Sirt3* mRNA, similar to previous data from microarrays (23), and Western blot analysis confirmed a parallel decrease of Sirt3 protein (Fig. 1*A*). Likewise, analysis of skeletal muscle from mice made obese by a chronic high-fat diet revealed a >50% decrease of *Sirt3* mRNA and protein compared with samples from mice fed a normal chow diet (Fig. 1*B*). Conversely, caloric restriction of mice for 12 wk resulted in a 2.5-fold increase of *Sirt3* mRNA and protein in skeletal muscle (Fig. 1*C*). By contrast, there was no change in muscle *Sirt3* expression level with aging as demonstrated by a comparison of 3- and 24-mo-old mice (Fig. S1).

Author contributions: E.J., E.M.V., and C.R.K. designed research; E.J., B.E., M.D.H., J.B., and K.Y.L. performed research; D.L. contributed new reagents/analytic tools; E.J., B.E., and M.D.H. analyzed data; and E.J. and C.R.K. wrote the paper.

The authors declare no conflict of interest.

[1]Present address: Department of Pathology and Institute of Gerontology, University of Michigan, Ann Arbor, MI 48109.

[2]To whom correspondence should be addressed. E-mail: c.ronald.kahn@joslin.harvard.edu.

This article contains supporting information online at www.pnas.org/lookup/suppl/doi:10.1073/pnas.1111308108/-/DCSupplemental.

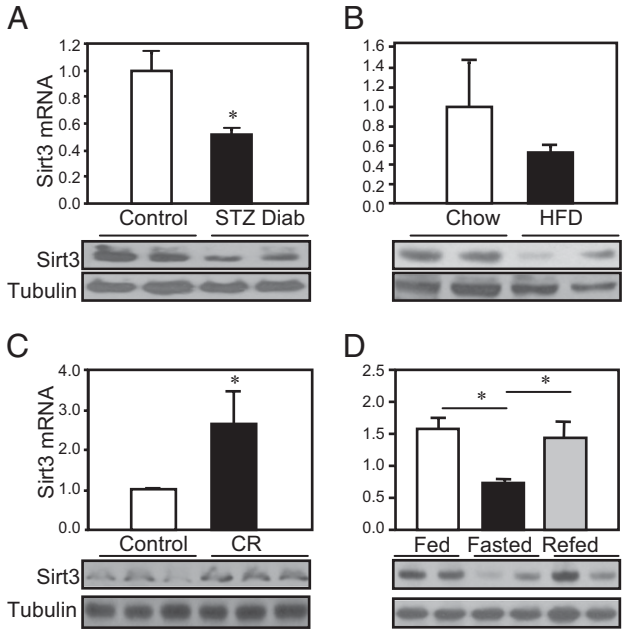

Fig. 1. Sirt3 expression in different states of diabetes and aging. (*A*) Skeletal muscles from the hind limbs of STZ diabetic mice and controls (8-wk-old C57BL/6) were collected. RNA and protein was extracted and analyzed by either quantitative PCR or Western blotting. (*B*) Skeletal muscles from the hind limb of obese high fat diet (HFD) and control mice were collected and processed for quantitative PCR and Western blot analysis for Sirt3 expression. (*C*) Hind-limb skeletal muscle of CR mice along with controls was collected and processed for quantitative PCR and Western blot analysis. (*D*) Mice were either randomly fed or fasted for 24 h; half of the fasted animals were then refed for 16 h. After each treatment, quadriceps muscles from fed, fasted, and refed groups were collected and processed for detection of Sirt3 expression as above.

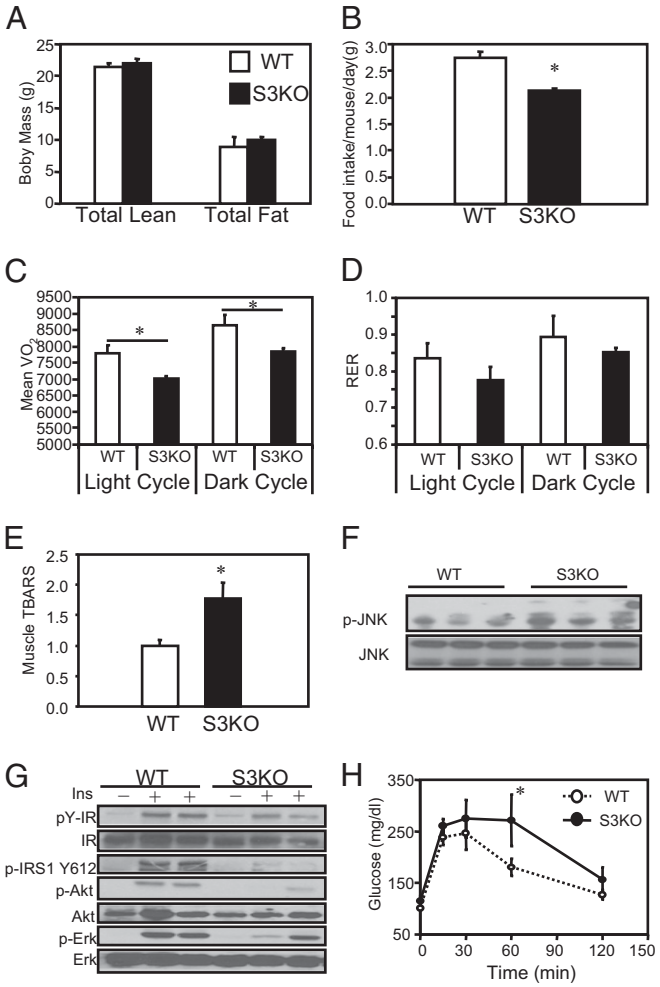

Fig. 2. Sirt3 knockout mice have increased oxidative stress and insulin resistance in skeletal muscle accompanied by decreased respiration. (*A*) A DXA scan was performed using 16-wk-old male C57BL/6 WT and KO mice ($n = 4$), body composition was measured, and Student's *t* test was performed for significance. (*B*) CLAMS analysis was performed using 16-wk-old male C57BL/6 WT and KO mice. Daily food intake per mouse over 48 h of CLAMS study was calculated and Student's *t* test was performed for significance. (*C*) VO_2 was recorded over 48 h and normalized for lean body mass calculated from the DXA scan. Dark cycle and light cycle VO_2 were analyzed separately and Student's *t* tests were performed for significance. (*D*) Dark cycle and light cycle RERs were calculated using the ratio between VCO_2 and VO_2. (*E*) Skeletal muscle from hind limbs of 24-wk-old fasted WT and Sirt3 KO mice was collected, and 25 mg of muscle was homogenized ($n = 5$). TBARS assay was performed with skeletal muscle homogenates using a TBARS assay kit (Calbiochem Inc.). Student's *t* test was performed for significance. (*F*) Hind-limb skeletal muscle from fed 24-wk-old male WT and Sirt3 KO mice was collected and processed and then subjected to Western blot analysis for JNK phosphorylation and total protein levels. (*G*) In vivo insulin stimulations were performed on 24-wk-old male WT and Sirt3 knockout mice via vena cava injection. Hind-limb skeletal muscle was collected, processed, and subjected to Western blot analysis using the indicated antibodies. (*H*) For GTTs, blood glucose was measured by tail bleeding at 0, 15, 30, 60, and 120 min after injection ($n = 5$).

Changes in *Sirt3* expression can also occur rapidly as illustrated by the effects of fasting and refeeding. After 24 h of fasting, *Sirt3* mRNA and protein expression in quadriceps muscle were decreased by ~50% and were reversed after refeeding for 16 h (Fig. 1*D*). The other mitochondrial sirtuin, *Sirt4*, was also down-regulated in *ob*/*ob* mice. During fasting, however, STZ-induced diabetes and caloric restriction had no effect on expression of Sirt4 in skeletal muscle (Fig. S2).

***Sirt3* Knockout Mice Exhibit Impaired Insulin Signaling and Increased Oxidative Stress in Skeletal Muscle.** To elucidate the metabolic effect of reductions in *Sirt3* on metabolism and insulin signaling, we used mice with targeted inactivation of the *Sirt3* gene. These mice had been backcrossed onto a C57BL/6 background for eight generations. Dual energy X-ray absortiometry (DXA) scanning of 20-wk-old male WT and Sirt3 KO mice revealed no differences in total, lean, or fat mass (Fig. 2*A*). Interestingly, despite identical body weight and composition, assessment in Comprehensive Lab Animal Monitoring System (CLAMS) chambers revealed that daily food intake was 20% lower in Sirt3 KO mice than in controls (Fig. 2*B*). This occurred with no change in activity (Fig. S3), but correlated with an ~10% decrease in basal oxygen consumption (VO_2) in Sirt3 KO mice in both dark and light cycles ($P < 0.05$) (Fig. 2*C*). There was also a trend for a reduced respiratory exchange rate (RER) (Fig. 2*D*), especially during the light cycle, suggesting decreased carbohydrate oxidation.

To determine if reduction of *Sirt3* in skeletal muscle might alter mitochondrial ROS production, we assayed thiobarbituric acid reactive substances (TBARS) in skeletal muscle homogenates of 24-wk-old male WT and *Sirt3* KO mice. This revealed a 75% increase in TBARS activity in the *Sirt3* KO mice (Fig. 2*E*), indicating elevated oxidative stress in skeletal muscle of KO mice. In parallel, the phosphorylation of JNK was increased ~50% in skeletal muscle of KO mice (Fig. 2*F*), reflecting activation of this stress kinase in *Sirt3*-deficient muscle.

To determine the effect of increased oxidative stress and JNK activation in *Sirt3* KO skeletal muscle on insulin signaling, we assessed insulin signaling in vivo by vena cava injection of insulin

(5 mU/g) into overnight fasted WT and *Sirt3* KO mice. Under basal and insulin-stimulated conditions, there were no significant differences in autophosphorylation of the skeletal muscle IR between WT and KO mice. By contrast, there was a >70% decrease in insulin-stimulated IRS-1 phosphorylation in *Sirt3* KO mice, which was paralleled by an ~50% reduction in insulin-stimulated Akt and Erk phosphorylation (Fig. 2*G*). This impaired insulin signaling in skeletal muscle was reflected at the whole-body level on i.p. glucose tolerance testing (GTT) with significantly higher glucose levels in the *Sirt3* KO mice at 60 min (Fig. 2*H*). Taken together, these data indicate that *Sirt3* knockout mice display impaired insulin action and a lower rate of oxygen consumption with increased oxidative stress in skeletal muscle.

***Sirt3* Knockdown Induces Insulin Resistance and Stress Kinase Activation.** To further mimic the decreased Sirt3 expression in different diabetes models, we used siRNA-mediated knockdown (KD) in cultured C2C12 myoblasts to assess the effects of reduced *Sirt3* on signaling. Western blotting revealed an over 90% decrease of Sirt3 protein in the *Sirt3* KD cells (Fig. 3*A*). Stimulation of serum-starved control and KD cells with 0, 10, and 100 nM insulin revealed no change in either basal or insulin-stimulated receptor autophosphorylation or receptor protein levels as assessed by Western blotting (Fig. 3*A*). However, insulin-stimulated tyrosine phosphorylation of IRS-1 was decreased by ~60%, with no significant change in the level of IRS-1 protein (Fig. 3*A*). As a result, downstream signaling events, including insulin-stimulated Akt and Erk phosphorylation, were decreased by 60–70% (Fig. 3*A*). Thus, the impaired insulin signaling in *Sirt3* knockdown C2C12 myoblasts is induced at the level of IRS-1 phosphorylation without affecting insulin receptor autophosphorylation or abundance.

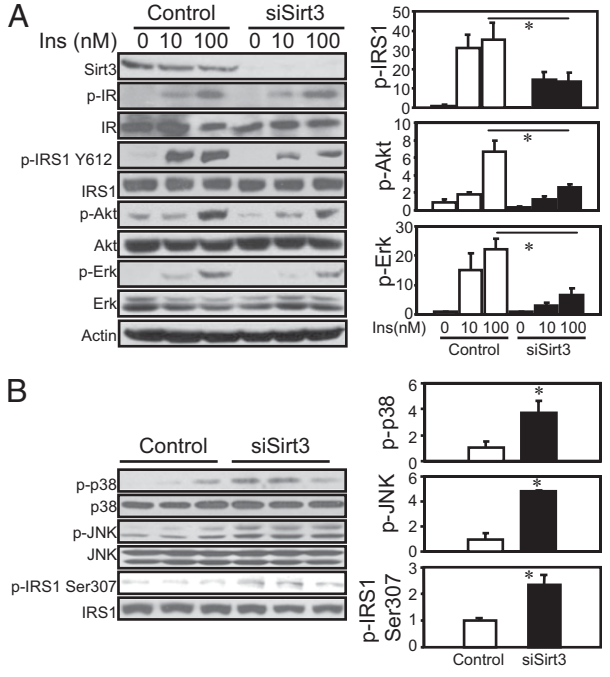

Fig. 3. Effects of Sirt3 knockdown on insulin sensitivity and stress kinase activation. (*A*) C2C12 cells were transiently transfected with siRNA targeting Sirt3 or scrambled control. Two days after transfection, cells were serum-deprived for 4 h and then stimulated by addition of different concentrations of insulin for 5 min. Cell lysate was collected and subjected to Western blotting with different antibodies. Autoradiography of Western blots was quantified with ImageJ software. The Student's *t* tests were performed for significance using relative units to serum-starved control results (n = 3). (*B*) Sirt3 knockdown and control cells were grown to 70% confluence with low glucose (100 mg/dL glucose) DMEM containing 10% FBS. Lysates were collected and processed and then subjected to Western blotting for antibodies against phosphorylated IRS-1, JNK, and p38 MAP Kinase, as well as antibodies against total proteins. The autoradiography was quantified by ImageJ software, and a Student's *t* test was performed for significance using relative units from the quantification (n = 3).

One potential link between reduction of mitochondrial Sirt3 and the insulin-signaling cascade could be oxidative stress created by mitochondrial dysfunction following reduction of *Sirt3*. Indeed, Western blot analysis of *Sirt3* KD cells in the basal state (100 mg/dL glucose in DMEM with 10% FBS) demonstrated two- to threefold increases in the stress-induced kinase p-38 mitogen-activated protein kinase and JNK phosphorylation compared with control (Fig. 3*B*). JNK has been shown to phosphorylate IRS-1 on serine 307 residue and to negatively regulate insulin signaling by reducing the IRS-1 tyrosine phosphorylation (24). Conversely, deletion of JNK in skeletal muscle has been shown to improve insulin sensitivity and prevent high-fat-diet–induced insulin resistance (14, 25). Consistent with this hypothesis, IRS-1 serine 307 phosphorylation was increased by twofold in *Sirt3* knockdown C2C12 myoblasts (Fig. 3*B*), indicating that *Sirt3* knockdown in C2C12 cells led to stress-induced kinase activation.

***Sirt3* Knockdown in C2C12 Myoblasts Induces Elevated Intracellular ROS and Oxidative Stress.** To directly assess the effect of *Sirt3* knockdown cells on intracellular ROS content, we treated cells with 5 (and 6)-chloromethyl-2′7′-dichlorodihydrofluorescein diacetate acetyl ester (CM-H2DCFDA) that monitors intracellular ROS concentrations. Quantification of mean fluorescence indicated a twofold increase in ROS levels in the Sirt3 KO cells (Fig. 4*A*, left pair of bars). H_2O_2 treatment of *Sirt3* KD cells further increased ROS levels, maintaining the twofold difference with the control cells under a stressed condition (Fig. 4*A*, right pair of bars).

The increased levels of ROS produced by oxidative stress are known to induce expression of multiple genes, including PGC-1α and GADD45 (26, 27). In parallel with the increased level of ROS in *Sirt3* KD cells, there were significant increases in expression of these genes in the basal state, and these were further enhanced after H_2O_2 treatment with no change in Sirt3 mRNA expression (Fig. 4*B*). *Sirt3* KD cells in the basal state also exhibited increased activities of the major ROS clearance enzymes with 25% and 40% increases in the activities of superoxide dismutase (SOD) and catalase (Fig. 4*C*). Thus, *Sirt3* KD cells produce more ROS, have increased levels of stress response genes, and have greater increases in enzyme activities involved in ROS clearance in response to the stress compared with control cells.

The increase in basal and H_2O_2-stimulated oxidative stress in *Sirt3* KD cells was associated with higher rates of cell death (Fig. 4*D*). When control cells were challenged with 1 mM H_2O_2 for 6 h, ~10% of the cells died, as assessed by trypan blue staining and cell counting. A similar challenge to *Sirt3* KD cells resulted in an increase to 25% dead cells (Fig. 4*D*). Treatment of WT C2C12 myoblasts with H_2O_2 or glucose oxidase also mimicked the effect of *Sirt3* KD with increased JNK phosphorylation (Fig. S4). Thus, knockdown of *Sirt3* in C2C12 myoblasts increases basal oxidative stress and makes cells more sensitive to oxidative challenges.

***Sirt3* Knockdown C2C12 Myoblasts Show Defects in Mitochondrial Respiration Capacity.** To better understand how *Sirt3* can affect mitochondrial function, we assessed the respiratory profile using a Seahorse Flux Analyzer of cells with stable knockdown of *Sirt3* and controls using an experimental paradigm with successive addition of blockers of different complexes in the mitochondrial electron transport chain. Changes on oxygen consumption rates were recorded, and areas under the curve (AUC) were calculated before and after each drug injection. Basal respiration, assessed as the oxygen consumption rate (OCR), revealed a small, but significant, ~15% decrease in *Sirt3* KD cells compared with control (Fig. 5*A*). Addition of the mitochondrial uncoupler

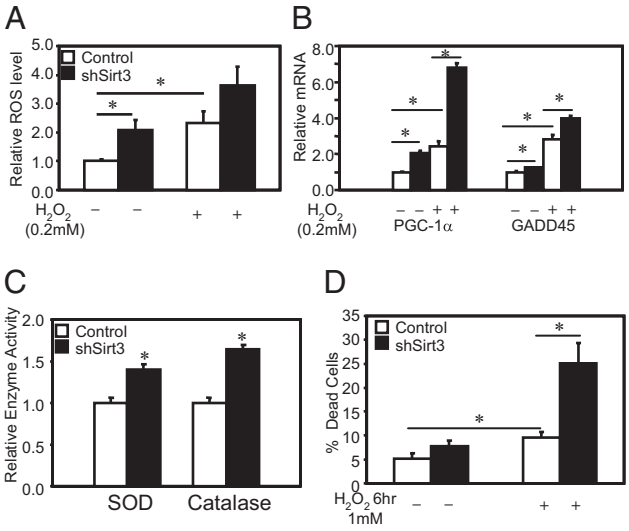

Fig. 4. Sirt3 knockdown C2C12 cells undergo stress response with elevated intracellular ROS production. (*A*) ROS levels of Sirt3 knockdown and control cells were determined using CM-H2DCFDA (Molecular Probes). (*B*) After incubation with media with or without 200 μM H_2O_2, intracellular ROS levels of both control and Sirt3 knockdown C2C12 cells were detected with 2.5 μM CM-H2DCFDA by flow cytometry. Using mean fluorescence of cells in either control or *Sirt3* KD cells under different conditions, Student's *t* test was performed for significance ($n = 4$). (*C*). Both control and *Sirt3* KD cells were incubated in low-glucose (100 mg/dL) DMEM containing 10% FBS with or without 200 μM H_2O_2 for 2 h following the oxidative challenge protocol that was previously described (26). Quantitative PCR was performed for different stress markers ($n = 3$). (*D*) Using cell homogenate, catalase activity assays were performed using catalase assay kit (Calbiochem). SOD activity assays were performed with cell homogenates using a SOD assay kit ($n = 4$; Cayman Chemical Company). Sirt3 knockdown and control cells were incubated with growth media with 1 mM of H_2O_2 for 6 h. At the end of the incubation period, all floating and attached cells were collected and resuspended in PBS. Aliquots of 20 μL of resuspended cells were stained with 20 μL 2× trypan blue and were subjected to cell counter analysis for trypan blue staining. The death rates of the cells were calculated on the basis of the percentage of trypan blue positive cells over the total cell number ($n = 5$).

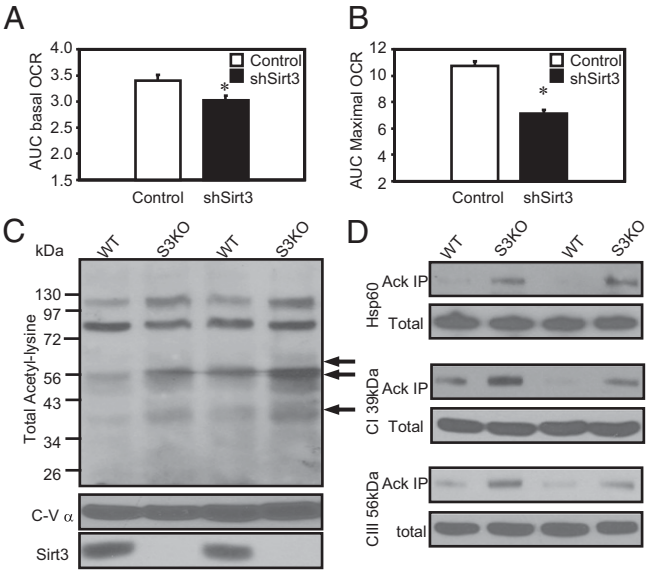

Fig. 5. Sirt3 knockdown cells display decreased basal and uncoupled rates OCR. (*A*) After the Seahorse Bioscience bioenergetic profiling experiment with mitochondrial uncoupler and inhibitors, basal mitochondrial respiration was calculated by subtraction of nonmitochondrial respiration (after rotenone injection) from total basal respiration (before oligomycin injection). (*B*) Uncoupled respiration stimulated by FCCP was calculated with AUC between the FCCP and rotenone injections. (*C*) Mitochondria from both WT and Sirt3 KO mice quadriceps muscles were isolated, and lysates were prepared for protein analysis as previously described (41). Western blot using mitochondrial total lysates was performed using anti-AcK antibody and antibodies against complex V subunit α and Sirt3. (*D*) The same mitochondrial lysates were immunoprecipitated with a polyclonal anti-AcK antibody (Cell Signaling Technology) and then subjected to Western blotting analysis using antibodies against a complex I 39-kDa subunit, a complex III core I subunit, and Hsp60.

Carbonyl cyanide 4-(trifluoromethoxy)phenylhydrazone (FCCP) (1 μM) to control cells increased OCR by three- to fivefold to 517 ± 43 pmol/min, reflecting maximum respiratory capacity, and this was decreased by ∼32% in the *Sirt3* KD cells to a maximum OCR of only 341 ± 42 pmol/min (Fig. 5*B*).

These decreases in basal and maximal respiratory capacity in *Sirt3* KD myoblasts occurred with no significant change in gene expression of a number of nuclear-encoded mitochondrial genes (Fig. S5). Likewise, there was no change in mitochondrial content as estimated by quantitative PCR of mitochondrial DNA-encoded NADH dehydrogenase 1 versus nuclear DNA-encoded β-globin (Fig. S6).

To identify potential targets of Sirt3 in mitochondria that might alter mitochondrial function in situations when Sirt3 levels are reduced, we assessed total mitochondrial protein acetylation status using lysates from skeletal muscle of either WT or *Sirt3* KO mice. Western blots of mitochondrial extracts using an anti–acetyl-lysine (anti-AcK) antibody revealed multiple acetylated mitochondrial proteins, with the most prominent bands at molecular weights of 96, 73, and 56 kDa and minor bands of 60, 50, and 40 kDa. Among these acetylated mitochondrial proteins, several (indicated by arrows in Fig. 5*C*) showed increased acetylation in skeletal muscle mitochondria lysates from the *Sirt3* KO mouse, suggesting that these may be targets of Sirt3 in skeletal muscle.

To begin to identify these candidate targets of Sirt3, we immunoprecipitated proteins from the mitochondrial extract using anti-AcK antibody and subjected the immunoprecipitate to SDS/PAGE and Western blotting with antibodies to specific mitochondrial proteins. Although Western blots of the total mitochondrial proteins extract revealed no differences between muscle of WT and *Sirt3* KO muscle in content of different subunits in the mitochondrial electron transporter chain (ETC) or the mitochondrial chaperon protein Hsp60, there were increased levels of the 39-kDa subunit of complex I, the 56-kDa core I subunit of complex III, and the 60-kDa Hsp60 precipitated by anti-AcK antibody from the *Sirt3* KO mitochondrial lysates (Fig. 5*D*). The increased acetylation on these ETC subunits and Hsp60 in *Sirt3* KO mitochondria suggests that they are direct substrates of Sirt3 and that changes in their acetylation status contribute to the altered the generation of mitochondrial ROS and response to oxidative stress (28–30).

Discussion

Mammals and other higher vertebrates express a family of sirtuins with different subcellular localizations and a wide range of substrate specificities. In this regard, *Sirt3*, *Sirt4*, and *Sirt5* are particularly interesting due to their mitochondrial localization, where they can regulate energy homeostasis and oxidative metabolism, as well as oxidative stress and cellular injury. In the present study, we find that *Sirt3* expression in skeletal muscle is significantly decreased in rodent models of type 1 and type 2 diabetes and is regulated by fasting and caloric restriction (CR). This led us to explore the link between skeletal muscle *Sirt3* expression and control of mitochondrial function and insulin sensitivity in diabetes. Using Sirt3 knockdown in C2C12 cells and skeletal muscles of Sirt3 KO mice, we show that decreases in Sirt3 expression lead to altered mitochondrial function with

increased levels of oxidative stress and activation of JNK, which in turn induces impaired insulin signaling.

Skeletal muscle is the major organ involved in postprandial glucose uptake and metabolism and peripheral insulin sensitivity. Changes in mitochondrial mass and oxidative phosphorylation have been shown to occur in muscle of individuals with diabetes and insulin resistance (31, 32). Mitochondrial dysfunction plays a major role in the onset of skeletal muscle insulin resistance through oxidative stress (33). Increased levels of oxidative stress have been demonstrated in skeletal muscle of type 2 diabetic mice (34) and in patients with diabetes (35). Antioxidant administration has been shown to decrease manifestations of insulin resistance in mice (36), but also to reduce the beneficial effects of exercise on muscle glucose uptake in humans in vivo (37), indicating the biphasic role of reactive oxygen species to both potentiate and inhibit insulin action.

Sirt3 provides a target for regulation of skeletal muscle insulin sensitivity via mitochondrial ROS production. Classically, ROS serve many important functions in cell defense, especially against microbial invasion. In recent years, ROS has also been shown to play important roles in activation of different signaling pathways and in the development of insulin resistance. At low physiological levels, ROS can mimic insulin action and enhance insulin sensitivity (37, 38). However, overproduction of ROS in pathological states can lead to adverse effects, including oxidative stress, inflammation, and insulin resistance. The ROS level in the cell is maintained by a balance between production and clearance. Our study shows that, despite increased catalase and SOD activity, ROS levels remain elevated in *Sirt3* KD cells. Thus, the increased level of ROS in knockdown cells is not due to decreased clearance or detoxification, but to overproduction of ROS with reduction of mitochondrial Sirt3 abundance and activity. Moreover, after treating control and Sirt3 KD C2C12 cells with antioxidants such as EU.K.134, which is a ROS scavenger, the difference in insulin-stimulated IRS-1 phosphorylation between control and Sirt3 KD cells was abolished, indicating that increased ROS level in KD cells induced impaired insulin signaling in these cells (Fig. S7).

The exact molecular mechanism by which *Sirt3* affects oxidative metabolism in skeletal muscle is still largely unknown. Recent studies have shown that *Sirt3* can serve as a broad-ranging mitochondrial deacetylase targeting many different substrates (18). Thus, identifying the specific targets regulated by reversible Sirt3 deacetylation that affect mitochondrial oxidative function and help maintain a normal cellular redox state and energy homeostasis will be challenging. Other recent reports have shown links between Sirt3 and mitochondrial ROS production by targeting HIF-1α and SOD2 under different pathological and physiological conditions (39, 40). By immunoprecipitating mitochondrial lysates from WT and KO muscle with anti–acetyllysine antibody, we have found that several proteins involved in the electron transporter chain are hyperacetylated in Sirt3 KO muscle, suggesting that these proteins may also be the direct targets of Sirt3. These include the 39-kDa subunit of complex I, the core I subunit of complex III, and the ATPase subunit α of complex V, as well as the chaperone protein Hsp60. Changes in acetylation of these proteins can potentially alter their activities and functions, leading to the mitochondrial stress response and ROS generation. Similar effects of Sirt3 deletion were also observed in tumor cells; ROS was generated from complex III of ETC which served as a signaling molecule that targeted protein functions in other cellular compartments (40). The acetylation of multiple mitochondrial proteins and their role as Sirt3 substrates also suggest that there are mitochondrial acetyl-transferases that can acetylate the targets of the Sirt3 deacetylase. These are also possible targets for alteration in diabetes.

One remaining question is how Sirt3 function is regulated under different pathological and physiological conditions. Although Sirt3 expression is decreased in fasting, it is elevated in muscle of CR mice, suggesting that short-term and chronic nutrient deprivation have different effects on Sirt3 activation. Furthermore, the global deletion of Sirt3 exhibits many other alterations in metabolism, such as altered oxygen consumption and decreased food intake, indicating that Sirt3 has important functions in other organs involved in metabolic homeostasis. It will be interesting to assess Sirt3's effects on appetite regulation in the hypothalamus, where neuronal signals involved in feeding behavior may be altered by deletion of Sirt3.

In summary, the decreased level of *Sirt3* in skeletal muscle in states of diabetes and obesity is an important component of the pathogenesis of type 2 diabetes, which can induce altered mitochondrial function, increase ROS production and oxidative stress, and lead to insulin resistance. Our data also provide direct evidence of the importance of reversible acetylation/deacetylation in the mitochondria and its potential role in development of insulin resistance and metabolic disorders. Agents that increase Sirt3 activity or expression could therefore potentially reverse at least some of the adverse effects of type 2 diabetes. Furthermore, site-specific deacetylation/acetylation of mitochondrial proteins may serve as a therapeutic tool to regulate cellular redox state and energy homeostasis in diabetes and insulin resistance, as well as other mitochondrial diseases.

Materials and Methods

Cell Culture and Maintenance. C2C12 cells (ATCC) were cultured in high-glucose (400 mg/dL) DMEM (Invitrogen) containing 10% FBS (Gemini Bioproducts) unless otherwise indicated. Cell media were replaced by low-glucose (100 mg/dL) DMEM containing 10% FBS 24 h prior to the experiments.

Animals. All animal studies were performed according to protocols approved by the Institutional Animal Care and Use Committee (Joslin Diabetes Center, Boston). Fed mice were killed at 9:00 AM or transferred to a new cage without food for 24 h and then killed for "fasted" studies. STZ diabetic mice were generated as previously reported (23). To induce obesity, mice were fed a high-fat diet (Teklad; TD.88137; 42% fat by calories) after weaning for 24 wk; low-fat diet controls were fed with a standard chow diet (Picolab Rodent Diet 20 containing 13.2% fat by calories). Studies used WT and *Sirt3*$^{-/-}$ C57BL/6 male mice, maintained on a standard chow diet, unless otherwise indicated.

Constructs and Generation of Transient/Stable *Sirt3* Knockdown Cells. *Sirt3* siRNA with scrambled control was purchased from IDT Technology for signaling and gene expression studies in C2C12 cells. Transient transfection of siRNA was achieved using Mirus Transit TKO transfection reagents. *Sirt3* shRNA and shGFP control lentiviral constructs were purchased from Open Biosystems, and stable Sirt3 knockdown cell lines were generated for ROS detection and Seahorse bioenergetics on oxygen consumption (OCR) studies.

Oxygen Consumption Analysis. Cellular OCR was measured using a Seahorse Bioscience XF24 analyzer. Cells were seeded at 30,000 cells/well 24 h before the analysis. Each experimental condition was analyzed using four to six biological replicates. Before measurement was taken, cells were washed, and 630 μL of sodium carbonate-free pH 7.4 DMEM was added to each well. After 15 min equilibration, three successive 2-min measurements were performed with intermeasurement mixing. A total of 70 μL of oligomycin (10 μM), FCCP (10 μM) or rotenone (10 μM) was injected into each well sequentially, and four to five successive 2-min measurements were performed with 2-min intermeasurement mixing. All OCR values before and after the injections and measurements were recorded, OCR and time curves where generated, and the AUC was calculated before and after each injection. For statistical analysis, Student's *t* test was performed between shGFP and shSirt3 C2C12 cells.

GTT and in Vivo Insulin Stimulation: For GTTs, mice were fasted overnight and then injected intraperitoneally with glucose (2 g/kg body weight). Tail-vein blood glucose measurements were performed at 0, 15, 30, 60, and 120 min after injection. For in vivo stimulation of insulin signaling, mice were fasted for 16 h and then anesthetized with an i.p. injection of pentobarbital (100 mg/kg). Insulin was injected (5 mU/g) through the inferior vena cava. After 5 min, skeletal muscles from the hind limbs were harvested. Muscles were ho-

mogenized and lysed at 4 °C, and lysates were subjected to Western blotting to assess insulin-stimulated phosphorylation cascades.

DEXAs Scanning and CLAM Testing. To assess metabolic effects of Sirt3 deletion in mice, body weight and composition were measured. Fat and lean mass was measured by DXA scanning. CLAMS method was used to measure activity level, food intake, volume of O_2 consumption, and volume of CO_2 production (Oxymax OPTO-M3 system; Columbus Instruments). Mean activity, VO_2, and VCO_2 of both WT and Sirt3 KO mice were calculated for dark and light cycles, and Student's *t* test was performed to determine statistical difference between metabolic measurements.

ACKNOWLEDGMENTS. We thank Dr. Marcelo Mori and Dr. Steven Russell for providing CR mice skeletal muscles. We also thank Dr. Stephane Gesta for active discussion and help with the Seahorse Bioscience analysis. The work was supported by research Grants R01DK33201 (to C.R.K) and R24DK085610 (to C.R.K and E.M.V.), a grant from the Ellison Foundation (to C.R.K.), and the Mary K. Iacocca Professorship. This study also received support from the Joslin Diabetes Endocrinology Research Center core laboratories.

1. DeFronzo RA, Tripathy D (2009) Skeletal muscle insulin resistance is the primary defect in type 2 diabetes. *Diabetes Care* 32(Suppl 2):S157–S163.
2. Martin BC, et al. (1992) Role of glucose and insulin resistance in development of type 2 diabetes mellitus: Results of a 25-year follow-up study. *Lancet* 340:925–929.
3. Kerouz NJ, Hörsch D, Pons S, Kahn CR (1997) Differential regulation of insulin receptor substrates-1 and -2 (IRS-1 and IRS-2) and phosphatidylinositol 3-kinase isoforms in liver and muscle of the obese diabetic (ob/ob) mouse. *J Clin Invest* 100:3164–3172.
4. Brozinick JT, Jr., Roberts BR, Dohm GL (2003) Defective signaling through Akt-2 and -3 but not Akt-1 in insulin-resistant human skeletal muscle: Potential role in insulin resistance. *Diabetes* 52:935–941.
5. Petersen KF, Shulman GI (2006) Etiology of insulin resistance. *Am J Med* 119 (5, Suppl 1):S10–S16.
6. Kelley DE, He J, Menshikova EV, Ritov VB (2002) Dysfunction of mitochondria in human skeletal muscle in type 2 diabetes. *Diabetes* 51:2944–2950.
7. Mootha VK, et al. (2004) Erralpha and Gabpa/b specify PGC-1alpha-dependent oxidative phosphorylation gene expression that is altered in diabetic muscle. *Proc Natl Acad Sci USA* 101:6570–6575.
8. Patti ME, et al. (2003) Coordinated reduction of genes of oxidative metabolism in humans with insulin resistance and diabetes: Potential role of PGC1 and NRF1. *Proc Natl Acad Sci USA* 100:8466–8471.
9. Perdomo G, et al. (2004) Increased beta-oxidation in muscle cells enhances insulin-stimulated glucose metabolism and protects against fatty acid-induced insulin resistance despite intramyocellular lipid accumulation. *J Biol Chem* 279:27177–27186.
10. Bruce CR, et al. (2008) Overexpression of carnitine palmitoyltransferase-1 in skeletal muscle is sufficient to enhance fatty acid oxidation and improve high fat diet-induced insulin resistance. *Diabetes* 58:550–558.
11. Simoneau JA, Kelley DE (1997) Altered glycolytic and oxidative capacities of skeletal muscle contribute to insulin resistance in NIDDM. *J Appl Physiol* 83:166–171.
12. Szendroedi J, et al. (2007) Muscle mitochondrial ATP synthesis and glucose transport/phosphorylation in type 2 diabetes. *PLoS Med* 4:e154.
13. Ragheb R, et al. (2009) Free fatty acid-induced muscle insulin resistance and glucose uptake dysfunction: Evidence for PKC activation and oxidative stress-activated signaling pathways. *Biochem Biophys Res Commun* 389:211–216.
14. Hirosumi J, et al. (2002) A central role for JNK in obesity and insulin resistance. *Nature* 420:333–336.
15. Kim JK, et al. (2004) PKC-theta knockout mice are protected from fat-induced insulin resistance. *J Clin Invest* 114:823–827.
16. Schwer B, North BJ, Frye RA, Ott M, Verdin E (2002) The human silent information regulator (Sir)2 homologue hSIRT3 is a mitochondrial nicotinamide adenine dinucleotide-dependent deacetylase. *J Cell Biol* 158:647–657.
17. Schwer B, Bunkenborg J, Verdin RO, Andersen JS, Verdin E (2006) Reversible lysine acetylation controls the activity of the mitochondrial enzyme acetyl-CoA synthetase 2. *Proc Natl Acad Sci USA* 103:10224–10229.
18. Lombard DB, et al. (2007) Mammalian Sir2 homolog SIRT3 regulates global mitochondrial lysine acetylation. *Mol Cell Biol* 27:8807–8814.
19. Ahn BH, et al. (2008) A role for the mitochondrial deacetylase Sirt3 in regulating energy homeostasis. *Proc Natl Acad Sci USA* 105:14447–14452.
20. Hirschey MD, et al. (2010) SIRT3 regulates mitochondrial fatty-acid oxidation by reversible enzyme deacetylation. *Nature* 464:121–125.
21. Shi T, Wang F, Stieren E, Tong Q (2005) SIRT3, a mitochondrial sirtuin deacetylase, regulates mitochondrial function and thermogenesis in brown adipocytes. *J Biol Chem* 280:13560–13567.
22. Bellizzi D, et al. (2005) A novel VNTR enhancer within the SIRT3 gene, a human homologue of SIR2, is associated with survival at oldest ages. *Genomics* 85:258–263.
23. Yechoor VK, et al. (2004) Distinct pathways of insulin-regulated versus diabetes-regulated gene expression: An in vivo analysis in MIRKO mice. *Proc Natl Acad Sci USA* 101:16525–16530.
24. Aguirre V, et al. (2002) Phosphorylation of Ser307 in insulin receptor substrate-1 blocks interactions with the insulin receptor and inhibits insulin action. *J Biol Chem* 277:1531–1537.
25. Sabio G, et al. (2009) Role of muscle JNK1 in obesity-induced insulin resistance. *Mol Cell Biol* 30:106–115.
26. St-Pierre J, et al. (2006) Suppression of reactive oxygen species and neurodegeneration by the PGC-1 transcriptional coactivators. *Cell* 127:397–408.
27. Edwards MG, et al. (2004) Impairment of the transcriptional responses to oxidative stress in the heart of aged C57BL/6 mice. *Ann NY Acad Sci* 1019:85–95.
28. Chun JN, et al. (2010) Cytosolic Hsp60 is involved in the NF-kappaB-dependent survival of cancer cells via IKK regulation. *PLoS ONE* 5:e9422.
29. Grivennikova VG, Vinogradov AD (2006) Generation of superoxide by the mitochondrial complex I. *Biochim Biophys Acta* 1757:553–561.
30. Guzy RD, Schumacker PT (2006) Oxygen sensing by mitochondria at complex III: The paradox of increased reactive oxygen species during hypoxia. *Exp Physiol* 91:807–819.
31. Befroy DE, et al. (2007) Impaired mitochondrial substrate oxidation in muscle of insulin-resistant offspring of type 2 diabetic patients. *Diabetes* 56:1376–1381.
32. Rabøl R, et al. (2010) Regional anatomic differences in skeletal muscle mitochondrial respiration in type 2 diabetes and obesity. *J Clin Endocrinol Metab* 95:857–863.
33. Anderson EJ, et al. (2009) Mitochondrial H2O2 emission and cellular redox state link excess fat intake to insulin resistance in both rodents and humans. *J Clin Invest* 119:573–581.
34. Yokota T, et al. (2009) Oxidative stress in skeletal muscle impairs mitochondrial respiration and limits exercise capacity in type 2 diabetic mice. *Am J Physiol Heart Circ Physiol* 297:H1069–H1077.
35. Ramakrishna V, Jailkhani R (2008) Oxidative stress in non-insulin-dependent diabetes mellitus (NIDDM) patients. *Acta Diabetol* 45:41–46.
36. Hildebrandt W, et al. (2004) Effect of thiol antioxidant on body fat and insulin reactivity. *J Mol Med (Berl)* 82:336–344.
37. Ristow M, et al. (2009) Antioxidants prevent health-promoting effects of physical exercise in humans. *Proc Natl Acad Sci USA* 106:8665–8670.
38. Loh K, et al. (2009) Reactive oxygen species enhance insulin sensitivity. *Cell Metab* 10:260–272.
39. Qiu X, Brown K, Hirschey MD, Verdin E, Chen D (2010) Calorie restriction reduces oxidative stress by SIRT3-mediated SOD2 activation. *Cell Metab* 12:662–667.
40. Bell EL, Emerling BM, Ricoult SJ, Guarente L (2011) SirT3 suppresses hypoxia inducible factor 1alpha and tumor growth by inhibiting mitochondrial ROS production. *Oncogene* 30:2986–2996.
41. Frezza C, Cipolat S, Scorrano L (2007) Organelle isolation: Functional mitochondria from mouse liver, muscle and cultured fibroblasts. *Nat Protoc* 2:287–295.